Spin-dependent tunneling in modulated structures of (Ga,Mn)As

P. Sankowski and P. Kacman
Institute of Physics, Polish Academy of Sciences, al. Lotników 32/46, PL 02-668 Warszawa, Poland

J. A. Majewski
Institute of Theoretical Physics and Interdisciplinary Center for Materials Modeling, Warsaw University, ul. Hoża 69, PL 00-681 Warszawa, Poland

T. Dietl
Institute of Physics, Polish Academy of Sciences and ERATO Semiconductor Spintronics Project, al. Lotników 32/46, PL 02-668 Warszawa, Poland
Institute of Theoretical Physics, Warsaw University, ul. Hoża 69, 00-681 Warszawa, Poland

(Dated: February 5, 2008)

A model of coherent tunneling, which combines multi-orbital tight-binding approximation with Landauer-Büttiker formalism, is developed and applied to all-semiconductor heterostructures containing (Ga,Mn)As ferromagnetic layers. A comparison of theoretical predictions and experimental results on spin-dependent Zener tunneling, tunneling magnetoresistance (TMR), and anisotropic magnetoresistance (TAMR) is presented. The dependence of spin current on carrier density, magnetization orientation, strain, voltage bias, and spacer thickness is examined theoretically in order to optimize device design and performance.

PACS numbers: 75.50.Pp, 72.25.Hg, 73.40.Gk

I. INTRODUCTION

Metallic magnetic tunnel junctions (MTJs) are important building blocks of the already existing spintronic devices, such as magnetic random access memories, magnetic heads, and sensors. The MTJ structure consists of ferromagnetic layers separated by a thin insulating barrier through which the carriers tunnel. The resistance of such a junction depends on the relative alignment of the magnetization vectors in the ferromagnetic layers, *i. e.*, the structure exhibits the tunnelling magnetoresistance (TMR) effect.

All-semiconductor MTJ structures offer potential for precise control of interfaces and barrier properties, particularly in the case of III-V compounds, for which epitaxial growth of complex heterostructures containing ferromagnetic (Ga,Mn)As or (In,Mn)As layers is especialy advanced.[1] Extensive studies of MTJs with (Ga,Mn)As ferromagnetic contacts carried out by various groups resulted in an increase of the observed TMR ratio from about 70% reported by Tanaka and Higo[2] to values higher than 250%.[3,4,5] Another key factor for developing novel functional semiconductor spintronic devices is an efficient electrical injection of spin polarized carriers. Here again the III-V ferromagnetic p-type semiconductor (Ga,Mn)As with its high spin polarization[6] appears as a promising material. The electrical spin injection from p-(Ga,Mn)As into non-magnetic semiconductor has first been achieved by injection of spin polarized holes.[7] Later, injection of spin polarized electrons was demonstrated employing interband tunneling from the valence band of (Ga,Mn)As into the conduction band of an adjacent n-GaAs in a Zener-Esaki diode.[8] Recently, a very high spin polarization of the injected electron current (*ca* 80%) was obtained in such devices.[9,10] It should be mentioned that both effects, the TMR and the spin polarization of tunneling current in the Zener-Esaki diode, decrease rapidly with the increase of the applied bias – a phenomenon observed also in the metallic TMR structures, and still not fully understood. Finally, it seems that TMR is sensitive to the direction of the applied magnetic field in respect to the direction of current and crystallographic axes. This so-called tunnel anisotropic magnetoresistance (TAMR) effect was observed in structures containing a single ferromagnetic electrode[11,12] as well as in typical TMR MTJ with two ferromagnetic contacts.[13,14]

These challenging experimental findings call for a theory that would describe the tunneling in semiconductor MTJs and would indicate the ways for optimized design of the devices. Since the ferromagnetic coupling in (Ga,Mn)As is mediated by the holes,[1,6] a meaningful theory has to take into account the entire complexity of the valence band, including the spin-orbit interaction. Furthermore, the intermixing of valence bands caused by spin-orbit coupling shortens the spin diffusion length and makes it comparable to the phase coherence length. This renders the models based on the classical spin-diffusion equation, which describe satisfactorily spin transport phenomena in metallic MTJs, non applicable directly to the structures containing layers of hole-controlled diluted ferromagnetic semiconductors.

The model of vertical transport in modulated structures of magnetic semiconductors described here combines the two-terminal Landauer-Büttiker formalism with the empirical multi-orbital tight-binding description of the semiconductor band structure. In this way,

the quantum character of spin transport over the length scale relevant for the devices in question is taken into account. Furthermore, the tight-binding approach, in contrast to kp models employed so-far,[15] allows for a proper description of effects crucial for spin transport in heterostructures such as atomic structure of interfaces, effects of Rashba and Dresselhaus terms as well as tunneling involving $\boldsymbol{k}$ states away from the center of the Brillouin zone. Our model has recently been applied to describe selected features of Zener-Esaki diodes[16,17] and TMR devices[17] as well as it was adopted to examine an intrinsic domain-wall resistance in (Ga,Mn)As.[18]

The remaining part of the present paper is organized as follows. In Section II we present our model, specifying the tight-binding parametrization, scattering formalism, and the way transfer coefficients are determined. In Section III, the calculated dependencies of spin polarization of the current in the Zener-Esaki diode on carrier density, trigonal distortion, and magnetization direction are shown and compared with available experimental findings. The calculated TMR and TAMR ratios for structures containing two ferromagnetic (Ga,Mn)As contacts, and their dependencies on the voltage bias, trigonal deformation, and on the width of non-magnetic spacer layer are presented and discussed in Section IV in reference to experimental results. Section V contains conclusions emerging from our work, particularly concerning possible optimizations of device performance.

II. THEORETICAL MODEL

We consider a prototype heterostructure, which is uniform and infinite in the x and y directions and has modulated magnetization along the z growth direction. The heterostructure is connected to two semi-infinite bulk contacts denoted by L and R and biased. In all cases considered, spin polarized carriers are injected from the ferromagnetic left lead. Our goal is to calculate the electric current in the structure and the degree of current spin polarization outside the left lead. Typical length of the studied structures is comparable to the phase coherence length. Therefore, we restrict ourselves to the vertical coherent transport regime that we treat within Landauer-Büttiker formalism, where the current is determined by the transmission probability from the ingoing Bloch state at the left contact to the outgoing Bloch state at the right contact. In the presence of spin-orbit coupling, the spin is not a good quantum number. The only preserved quantities in tunneling are the energy E and, due to spatial in-plane symmetry of our structures, the in-plane wave vector $\boldsymbol{k}_{\|}$. We use semi-empirical tight-binding formalism to calculate electronic states of the system for given $\boldsymbol{k}_{\|}$ and E and further to compute transmission coefficients.

A. Tight-binding model

First, we describe the construction of the tight-binding Hamiltonian matrix for 'normal' GaAs and AlAs as well as ferromagnetic (Ga,Mn)As layers of the heterostructure. To describe the band structure of the bulk GaAs and bulk AlAs, we use the nearest neighbor (NN) $sp^3d^5s^*$ tight-binding Hamiltonian (resulting in 20 spin-orbitals for each anion or cation), with the spin-orbit coupling included.[19] This model reproduces correctly the effective masses and the band structure of GaAs and AlAs in the whole Brillouin zone. With the tight-binding Hamiltonian introduced above, each double layer (cation + anion) is represented by 40×40 matrix. It should be pointed out that the d orbitals used in our $sp^3d^5s^*$ parametrization are not related to the 3d semi-core states and are of no use for description of Mn ions incorporated into GaAs. The presence of Mn ions in (Ga,Mn)As is taken into account by including the sp-d exchange interactions within the virtual-crystal and mean-field approximations. In the spirit of the tight-binding method, the effects of an external interaction are included in the on-site diagonal matrix elements of the tight-binding Hamiltonian. Here, the shifts of on-site energies caused by the sp-d exchange interaction are parameterized in such a way that they reproduce experimentally obtained spin splitting: $N_0\alpha = 0.2$ eV of the conduction band and $N_0\beta = -1.2$ eV of the valence band.[20] It should be, however, mentioned that since we neglect exchange interactions between the holes, the valence spin splitting is presumably underestimated by about 20%.[6] The other parameters of the model for the (Ga,Mn)As material and for the NN interactions between GaAs and (Ga,Mn)As are taken to be the same as for GaAs. This is well motivated because the valence-band structure of (Ga,Mn)As with small fraction of Mn has been shown to be quite similar to that of GaAs.[20] Consequently, the valence band offset between (Ga,Mn)As and GaAs originates only from the spin splitting of the bands in (Ga,Mn)As. The Fermi energy in the constituent materials is determined by the assumed carrier concentration and is calculated from the density of states obtained for tight-binding Hamiltonian. Our calculations of the Fermi energy for various hole concentrations are consistent with the corresponding results presented in Ref. 6. Having determined the Hamiltonian of the system, we are now in the position to define the current and current spin polarization in the presence of spin-orbit coupling.

B. Current and current spin polarization

For a given energy E and in-plane wave-vector $k_{\|}$, the Bloch states in the left L and right R leads (i and j, respectively) are characterized by the wave vector component $k_{\perp}$ perpendicular to the layers and are denoted by $|L, k_{L,\perp,i}\rangle$ and $|R, k_{R,\perp,j}\rangle$, respectively. The indices i and j indicate all possible pairs for 40 bands described by

the tight-binding Hamiltonian. The transmission probability $T_{L,k_{L,\perp,i}\to R,k_{R,\perp,j}}$ is a function of the transmission amplitude $t_{L,k_{L,\perp,i}\to R,k_{R,\perp,j}}(E,\boldsymbol{k}_\parallel)$ and group velocities in the left and right lead, $v_{L,\perp,i}$ and $v_{R,\perp,j}$

$$T_{L,k_{L,\perp,i}\to R,k_{R,\perp,j}}(E,\boldsymbol{k}_\parallel) = \\ = \left|t_{L,k_{L,\perp,i}\to R,k_{R,\perp,j}}(E,\boldsymbol{k}_\parallel)\right|^2 \frac{v_{R,\perp,j}}{v_{L,\perp,i}}. \quad (1)$$

The current flowing in the right direction can now be written as[21]

$$j_{L\to R} = \frac{-e}{(2\pi)^3\hbar}\int_{BZ} d^2k_\parallel dE f_L(E) \\ \sum_{\substack{k_{L,\perp,i},k_{R,\perp,j}\\ v_{L,\perp,i},v_{R,\perp,j}>0}} T_{L,k_{L,\perp,i}\to R,k_{R,\perp,j}}(E,\boldsymbol{k}_\parallel), \quad (2)$$

where f_L or respectively f_R are the electron Fermi distributions in the left and right interface and i,j number the corresponding Bloch states. Plugging in the expresion given in Eq. 1 and using the time reversal symmetry

$$T_{L,k_{L,\perp,i}\to R,k_{R,\perp,j}}(E,\boldsymbol{k}_\parallel) = \\ = T_{L,-k_{R,\perp,j}\to R,-k_{L,\perp,i}}(E,\boldsymbol{k}_\parallel) \quad (3)$$

we get

$$j = \frac{-e}{(2\pi)^3\hbar}\int_{BZ} d^2k_\parallel dE\,[f_L(E)-f_R(E)] \\ \sum_{\substack{k_{L,\perp,i},k_{R,\perp,j}\\ v_{L,\perp,i},v_{R,\perp,j}>0}} \left|t_{L,k_{L,\perp,i}\to R,k_{R,\perp,j}}(E,\boldsymbol{k}_\parallel)\right|^2 \frac{v_{R,\perp,j}}{v_{L,\perp,i}}. \quad (4)$$

Let us define the spin polarization of the outgoing Bloch state, in respect to magnetization direction in the source lead

$$P_{R,k_{R,\perp,i}}(E,\boldsymbol{k}_\parallel) = \langle R,k_{R,\perp,i}|\vec{\Omega}\cdot\vec{s}|R,k_{R,\perp,i}\rangle, \quad (5)$$

where $\vec{\Omega}$ is the magnetization direction vector and $\vec{s}$ is the spin operator. Then, we can define the spin polarized current

$$j_s = \frac{-e}{(2\pi)^3\hbar}\int_{BZ} d^2k_\parallel dE\,[f_L(E)-f_R(E)] \\ \sum_{\substack{k_{L,\perp,i},k_{R,\perp,j}\\ v_{L,\perp,i},v_{R,\perp,j}>0}} T_{L,k_{L,\perp,i}\to R,k_{R,\perp,j}}(E,\boldsymbol{k}_\parallel)P_{R,k_{R,\perp,i}}. \quad (6)$$

The spin polarization of the coherently transmitted current is now equal to

$$P_s = \frac{j_s}{j}. \quad (7)$$

To calculate the current one has to determine the transmission probability, thus the transmission amplitude $t_{L,k_{L,\perp,i}\to k_{R,R,\perp,j}}(E,\boldsymbol{k}_\parallel)$ and the group velocities $v_{L,\perp,j}$ of the ingoing and $v_{R,\perp,j}$ of outgoing states. These can be obtained by solving the Schrödinger equation for the structure with the appropriate scattering boundary conditions. In our studies, we follow closely the procedure detailed in Refs. 22 and 23, which we have generalized to the case with spin-orbit coupling.

III. SPIN-DEPENDENT ZENER TUNNELING

A. Effect of carrier densities

The rather high $\approx 80\%$ spin polarization of the tunneling current, obtained recently in Zener-Esaki diodes[9,10] opens new perspectives for applications of electron spin injection. The degree of current spin polarization decreases sharply with the bias,[9,10] an effect explained quantitatively by our model.[16] On the other hand, it is well known that magnetic characteristics of (Ga,Mn)As depend strongly on both hole and manganese concentrations and that (Ga,Mn)As films exhibit a variety of anisotropic properties.[6,24,25] It is thus obvious that the degree of spin polarization of the tunneling current may depend on these intrinsic features of (Ga,Mn)As layers. Indeed, we have already shown[17] that a higher content of magnetic ions x in $Ga_{1-x}Mn_xAs$ results in an increase of the spin polarization of the tunneling current. In contrast, an opposite change was obtained when the hole concentration was increased.

In order to get a better insight into processes controlling spin polarization of the current, we have examined the dependence of tunneling on the in-plane wave vector in the low bias limit. As shown in Fig. 1(a), the total current is dominated by the tunneling from states close to the Γ point. This is because in the tunneling process the in-plane components of $\boldsymbol{k}_\parallel$ wave vectors are conserved, *i. e.*, they have to match to the small $\boldsymbol{k}_\parallel$ vectors at the Fermi level in the conduction band of n-type GaAs ($n = 10^{19}$ cm^{-3}). Turning to current spin polarization, we note that it decreases with the hole concentration p because the higher p the smaller is the spin polarization at the Fermi level in the vicinity of the center of the Brillouin zone. This is shown in Fig. 2 where the cross sections of the Fermi sphere for different hole concentrations in p-$Ga_{0.92}Mn_{0.08}As$ with the saturated value of magnetization are presented. At the same time we find that the large $\boldsymbol{k}_\parallel$ vectors are responsible for the spin polarization of the current, as depicted in Fig. 1(b). This suggests that a higher concentration of electrons in n-GaAs layer should result in matching of the larger k vectors and thus in higher spin polarization of the current. Indeed, when the electron concentration is increased from $n = 10^{19}$ cm^{-3} to $n = 10^{20}$ cm^{-3}, the current spin polarization becomes higher by about 8%.

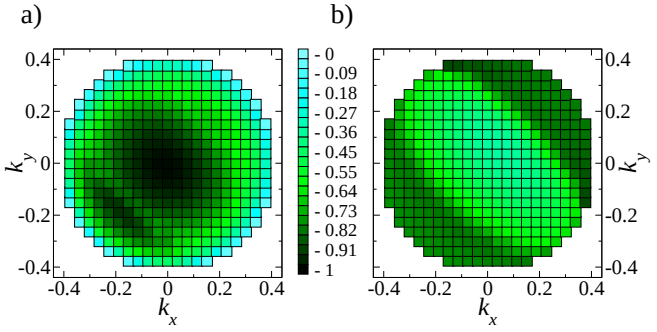

FIG. 1: [color on-line] Dependence of tunneling current (a) and its spin polarization (b) on the in-plane wave vector in p-$Ga_{1-x}Mn_xAs$/n-GaAs Zener-Esaki diode in the limit of low bias. The calculation was performed for the hole concentration $p = 3.5 \times 10^{20}$ cm^{-3}, electron concentration $n = 10^{19}$ cm^{-3}, and the saturated magnetization corresponding to the Mn content $x = 0.08$.

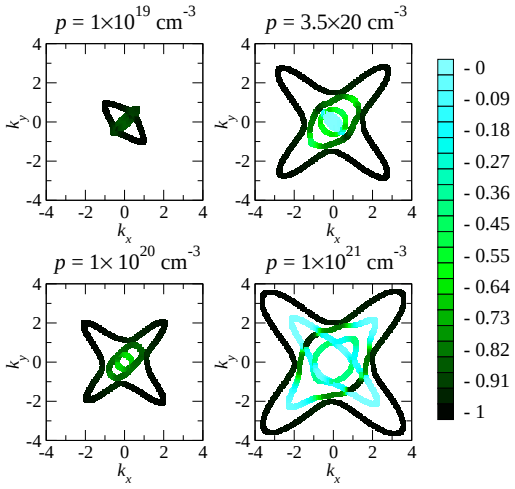

FIG. 2: [color on-line] Cross section of the valence bands at the Fermi energy for various hole concentrations p in p-$Ga_{0.92}Mn_{0.08}As$. Color scale denotes spin polarization. Magnetization is taken along the [110] direction.

B. Anisotropic Zener tunneling - in-plane magnetization

In this and next subsection we asses the importance of a new mechanism called tunneling anisotropic magnetoresistance (TAMR). This effect consists of a change in the tunnel resistance upon the rotation of magnetization. The phenomenon, recently discovered in structures with a single (Ga,Mn)As ferromagnetic layer,[11,12] results from the fact that tunneling resistance depends on the relative orientation of magnetization in respect to the direction of current and crystallographic axes. This is due to the strong spin-orbit coupling and the highly anisotropic Fermi surface in (Ga,Mn)As (compare Fig. 2) – it is why TAMR was not reported for structures based on ferromagnetic metals, where typically spin-orbit characteristic energies are smaller than the Fermi energy.

We consider a simple junction consisting of several layers of p-type $Ga_{1-x}Mn_xAs$, $x = 0.08$, $p = 3.5 \times 10^{20}$ cm^{-3}, followed by several layers of n-type GaAs, $n = 10^{19}$ cm^{-3} in the weak bias limit. Interestingly, as shown in Fig. 3 the model reveals that the current magnitude and its spin polarization differ for magnetization along [110] and along [$\bar{1}$10] crystallographic axis, even in the absence of any extrinsic deformation. This reflects the asymmetry of the (Ga,Mn)As/GaAs interface, at which the [110] and [$\bar{1}$10] directions are not equivalent, so that the T_d symmetry of the zinc-blende crystal is reduced to C_{2v} for the heterostructure in question. Actually, a 6% difference in spin polarization of the current for the unstrained structure, which is visible in Fig. 3(b), agrees with that observed experimentally.[16]

The intrinsic anisotropy of the Zener tunneling current depends on the hole concentration, as shown in Fig. 4. The change in the tunneling current upon rotation of the magnetization vector from [110] to [$\bar{1}$10] direction increases with the decrease of hole concentration, reaching 8.5% for $p = 1 \times 10^{19}$ cm^{-3}. Such a low hole concentration can, in fact, correspond to a depletion region in the p-(Ga,Mn)As/n-GaAs junction,[13,14] though hole localization may render our theory invalid in this low hole concentration range. Thus, our model predicts for (Ga,Mn)As/GaAs Zener diodes an in-plane TAMR magnitude of the order of several percents without assuming any extrinsic strain. Although the obtained TAMR value agrees with the observation reported in Ref. 11, it should be emphasized that in that experiment (Ga,Mn)As/AlO_x/Au tunnel junction was examined. Moreover, the symmetry of the experimental TAMR effect implies the existence of an extrinsic deformation breaking the equivalence of [100] and [010] crystallographic axes.

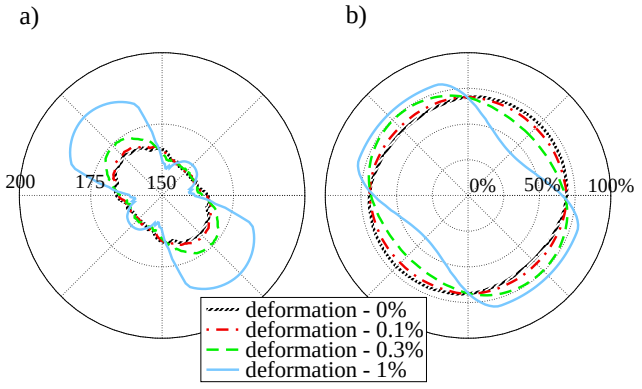

FIG. 3: [color on-line] Dependence of Zener tunneling current (a) and its spin polarization (b) on the direction of in-plane magnetization without strain and for deformations up to 1% applied along the [110] axis. Calculations performed for Mn content $x = 0.08$, hole concentration $p = 3.5 \times 10^{20}$ cm^{-3}, and electron concentration $n = 10^{19}$ cm^{-3}.

Typically (Ga,Mn)As films exhibit uniaxial anisotropy,

whose character implies the presence of an extrinsic trigonal distortion along the [110] axis.[25] A strain as small as 0.05% was found to explain the magnitude of the corresponding uniaxial in-plane anisotropy field.[25] The effect of the trigonal strain on the Zener current and its spin polarization is presented in Fig. 3 together with previously discussed results for unstrained structures. As seen, the strain causes an additional in-plane anisotropy. However, a rather strong deformation is needed to obtain a significant dependence of spin current polarization on the direction of the magnetization vector. Even for 0.1% deformation, which is two times larger than that evaluated in Ref. 25, the anisotropy of the spin polarization of the current is still very small. When a strong, 1%, deformation is assumed, the calculation predicts a 10% increase of current spin polarization for magnetization along $[\bar{1}10]$ axis. At the same time, the obtained spin polarization for the magnetization along [110] direction is smaller by about 30%.

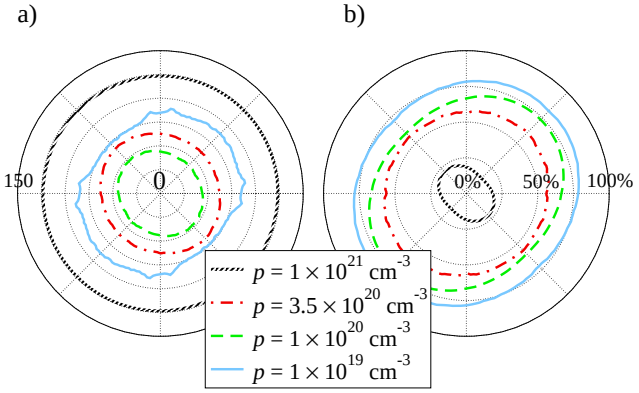

FIG. 4: [color on-line] Dependence of Zener tunneling current (a) and its spin polarization (b) on the direction of in-plane magnetization for various hole concentrations; Mn content $x = 0.08$ and electron concentration $n = 10^{19}$ cm^{-3}.

C. Anisotropic Zener tunneling - out-of-plane magnetization

The spin dependent interband tunneling is sensitive not only to the in-plane magnetization direction. It has been shown in Ref. 12 that rotation of magnetization by applying an out-of-plane magnetic field leads also to a TAMR signal in a Zener-Esaki diode. The magnitude of perpendicular tunneling anisotropic magnetoresistance is defined as

$$TAMR_{\perp} = \frac{R(H_{\perp}) - R(0)}{R(0)}, \qquad (8)$$

where R($H_{\perp}$) and R(0) are the resistances for two mutually perpendicular, out-of-plane and in-plane configurations of saturated magnetization, *i. e.*, for magnetization along [001] and [100] crystallographic axis, respectively. It is worth noting that under the presence of spin-orbit interaction, a relatively large change in resistance is expected when the direction of magnetization alternates from perpendicular to parallel in respect to the current, even if the effect of epitaxial strain, which makes the [100] and [001] directions non-equivalent, is disregarded. In the Boltzmann conductance regime, the effect is known as anisotropic magnetoresistance (AMR), and has already been studied in (Ga,Mn)As experimentally and theoretically.[26]

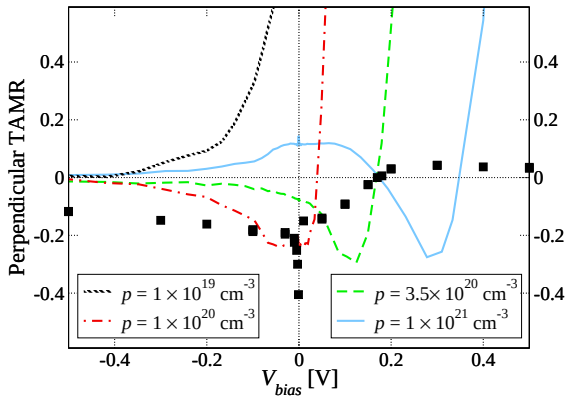

FIG. 5: [color on-line] The bias dependence of the relative change in the tunneling resistance in Zener-Esaki p-$Ga_{0.94}Mn_{0.06}As$/n-GaAs diode when magnetization is rotated out-of-the-plane, for various hole concentrations; $n = 10^{19}$ cm^{-3}. The black squares are experimental points from Ref. 12.

The calculated relative changes of the structure resistance for the magnetization vector flipping between perpendicular-to-the-plane and in-plane directions are shown in Fig. 5 as a function of bias for various hole concentrations in $Ga_{0.94}Mn_{0.06}As$. For $p = 3.5 \times 10^{20}$ cm^{-3}, the maximum of the computed TAMR effect, exceeding 20%, is seen at small bias voltages. These results are compared with the experimental findings of Ref. 12, where the structure containing ferromagnetic $Ga_{0.94}Mn_{0.06}As$ with $T_C \approx 70$ K was studied. According to the p-d Zener model,[6] such a value of T_C corresponds to $p \approx 10^{20}$ cm^{-3}.

We see in Fig. 5 that the theory describes correctly the experimental magnitude of $TAMR_{\perp}$ for small bias at both polarizations. We see also that the computed $TAMR_{\perp}$ tends to vanish with the increase of the reverse bias, whereas when the forward bias is assumed, $TAMR_{\perp}$ changes sign and tends to infinity. Such change of sign for the forward bias is also revealed experimentally, but the measured $TAMR_{\perp}$ appears to vanish for higher values of positive bias. This inconsistency can be explained by recalling that the computed tunneling current stops to flow above the tunneling cutoff voltage, which is determined by a sum of the energy distance from the hole Fermi level E_F^v to the top of the valence band in (Ga,Mn)As and the energy difference between the bottom of the conduction band and electron Fermi level E_F^c in GaAs. In the experiment, however, some current related to band-gap states

appears to dominate near the cutoff voltage. In turn, series bulk resistances, which are not taken into account in the calculations, may dominate at high reverse bias. Accordingly, standard AMR appears to contribute to the experimental value of $TAMR_\perp$ in this bias regime.[12]

Figure 5 shows also the $TAMR_\perp$ calculated for different hole concentrations in the magnetic layer. Due to the strong p-d exchange and large spin splitting in the (Ga,Mn)As valence band, for the low value $p = 1 \times 10^{19}$ cm^{-3} all spin subbands above the Fermi energy have the same spin polarization and thus $TAMR_\perp$ does not change the sign upon applying the positive bias. When, however, the Fermi level is very deep in the band, in the case of large $p = 1 \times 10^{21}$ cm^{-3}, different spin subbands contribute to the current for various voltages and $TAMR_\perp$ as a function of bias changes the sign twice.

IV. TUNNELING MAGNETORESISTANCE

A. Bias dependence

In the previous section, we have used the model to consider a device with just one interface between magnetic (Ga,Mn)As and nonmagnetic GaAs. The typical tunneling magnetoresistance (TMR) devices are, however, more complicated – they consist of a trilayer structure with two such interfaces, for instance, two magnetic p-type $Ga_xMn_{1-x}As$ contacts separated by a nonmagnetic GaAs barrier. In such structures a strong TMR effect, *i. e.*, a large difference in the resistance of the device for two configurations: parallel (ferromagnetic – FM) and the antiparallel (antiferromagnetic – AFM) alignments of magnetizations in the contacts, has been observed.[2,4,5] The TMR value is usually described by the ratio,

$$\mathrm{TMR} = \frac{R_{\mathrm{FM}} - R_{\mathrm{AFM}}}{R_{\mathrm{AFM}}}, \qquad (9)$$

where R_{FM} and R_{AFM} are the structure resistances for the FM and AFM configuration, respectively. Similarly to the spin polarization of the tunneling current in Zener-Esaki diode, TMR increases with the content of the magnetic ions and decreases with the concentration of the holes in (Ga,Mn)As layers.[17] Unfortunately, in all experiments the observed TMR shows a rapid and hitherto unexplained decay with the increase of the applied bias. As shown in Fig. 6, our calculations reproduce such decay. This suggests that the dependence of TMR on the applied bias results predominantly from the band structure effects in this case.

In Fig. 6(a) one should note a strong dependence of TMR and its decay with applied voltage on the hole concentration in the magnetic contacts. However, one can also see that the hole concentration does not influence very strongly the bias where the TMR reaches zero. This voltage, ca 0.3 V, corresponds to the valence band offset between $Ga_{0.92}Mn_{0.08}As$ and GaAs, which is determined by the spin splitting in the valence band of the former.

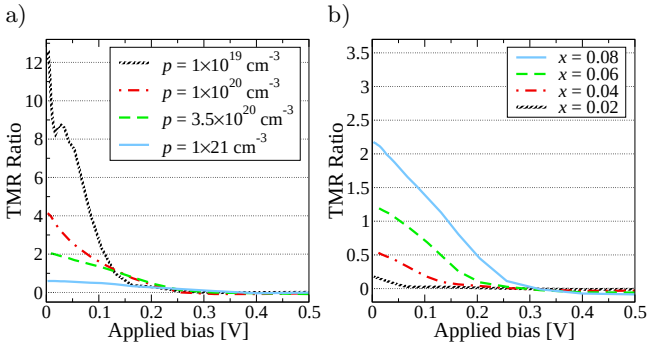

FIG. 6: [color on-line] The calculated bias dependence of the TMR effect in p-$Ga_{1-x}Mn_xAs$/$(GaAs)_4$/p-$Ga_{1-x}Mn_xAs$ trilayer (with the GaAs barrier width $d = 4$ monolayers) for various hole concentrations p and Mn ions content $x = 0.08$ (a) and for various values of x and $p = 3.5 \times 10^{20}$ cm^{-3} (b).

The presented in Fig. 6(b) TMR ratios for the magnetic contacts with various Mn content, *i e.*, with different spin splitting, confirms this conclusion. These results suggest that the TMR and its decrease with the applied bias can be controlled by appropriate engineering of the band offsets in the heterostructure, in particular, by a proper choice of the nonmagnetic barrier. To check this prediction theoretically, we replace in the calculations the GaAs by AlAs, which produces a higher by 0.55 V barrier for the holes. The results presented in Fig. 7 show that, indeed, for tunneling through the AlAs barrier, the TMR magnitude decreases with the bias much slower than in the case of GaAs. Moreover, for a higher tunneling barrier one can expect also higher TMR ratios.

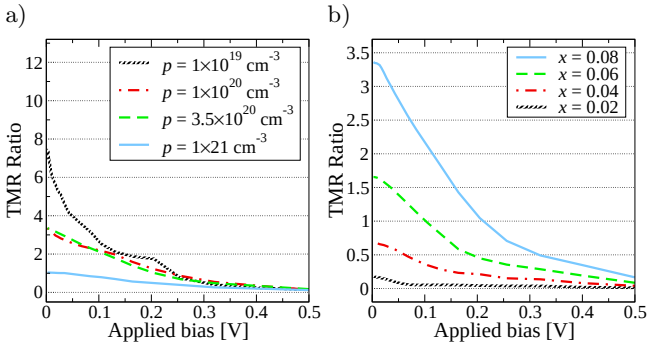

FIG. 7: [color on-line] The bias dependence of the TMR ratio for p-$Ga_{1-x}Mn_xAs$/$(AlAs)_4$/p-$Ga_{1-x}Mn_xAs$ with $x = 0.08$ and various hole concentrations (a); for various values of x and $p = 3.5 \times 10^{20}$ cm^{-3} (b).

A related behavior can be seen in the study of the dependence of the TMR effect on the width of the barrier, presented in Fig. 8. In agreement with experimental observations,[2] the calculated TMR drops rapidly when the barrier becomes wider. However, for AlAs which forms a higher barrier, the decrease of the TMR ratio with the number of barrier monolayers is much weaker.

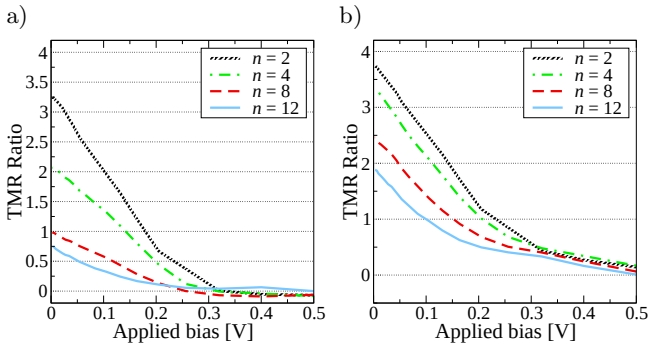

FIG. 8: [color on-line] The bias dependence of the TMR ratio for various thicknesses d of the barrier layer in (a) p-$Ga_{0.92}Mn_{0.08}As$/$(GaAs)_d$/p-$Ga_{0.92}Mn_{0.08}As$; (b) p-$Ga_{0.92}Mn_{0.08}As$/$(AlAs)_d$/p-$Ga_{0.92}Mn_{0.08}As$

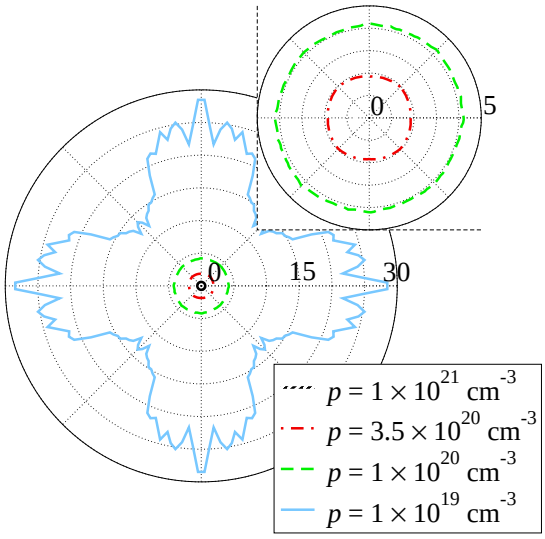

FIG. 9: [color on-line] Dependence of TMR ratio on the direction of in-plane magnetization for various hole concentrations in p-$Ga_{0.92}Mn_{0.08}As$/$(GaAs)_4$/p-$Ga_{0.92}Mn_{0.08}As$ trilayer structure.

B. Anisotropy of tunneling magnetoresistance

The calculated dependence of TMR on the in-plane direction of the magnetization vector is shown in Fig. 9. It is seen that in the case of TMR the [100] and [110] magnetization directions remains not equivalent, while TMR is identical for [110] and [$\bar{1}$10]. Thus, the D_{2d} symmetry is recovered if two interfaces are involved, in contrast to the case of spin current polarization in the Esaki-Zener diode, where C_{2v} symmetry of a single zinc-blende interface led to the non-equivalence of the [110] and [$\bar{1}$10] directions, as discussed in the previous section.

As shown in Fig. 9, the in-plane anisotropy of TMR depends crucially on the hole concentration in the magnetic layer. For hole concentrations p in the range of 10^{20} cm^{-3} the obtained anisotropy of TMR is below 10%, however, for low concentrations, $p = 10^{19}$ cm^{-3}, it becomes as strong as 250%. The reason for this behavior becomes clear when we look at Fig. 10 that shows the dependence of the tunneling current in the AFM configuration on the in-plane wave vector for different directions of magnetization. In Fig. 10(a), *i. e.*, in the case of $p = 10^{19}$ cm^{-3} the region of the Brillouin zone that takes part in the tunneling is strongly dependent on the magnetization direction, in contrast to the results for higher hole concentrations presented in Fig. 10(b). It should be stressed that such behavior has been obtained only for the AFM alignment. The calculated tunneling current in the FM configuration does not virtually depend on the direction of magnetization – only a very small difference between [110] and [010] direction has been found.

A similar effect can be also noticed in the calculated dependence of the TMR ratio on strain, as shown in Fig. 11. Here again we see that upon trigonal strain the tunneling current becomes anisotropic only for the AFM alignment of magnetization in the two magnetic contacts.

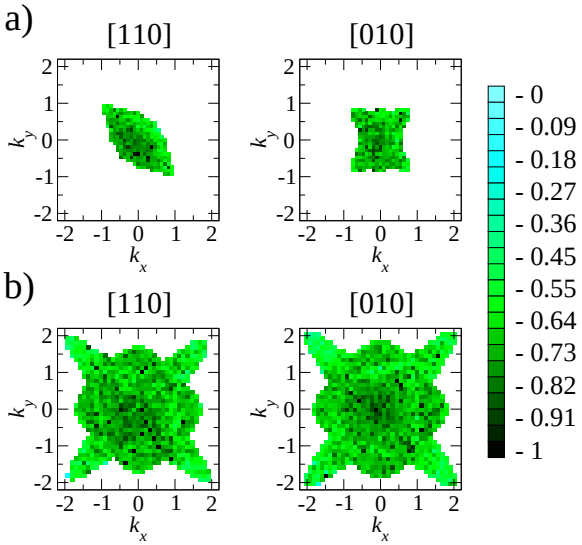

FIG. 10: [color on-line] Dependence of tunneling current on the direction of the in-plane wave vector for antiparallel configuration of magnetizations (AFM) along the [110] and [010] crystallographic directions, as indicated in the plots, and for hole concentrations 1×10^{19} cm^{-3} (a) and 3.5×10^{20} cm^{-3} (b).

C. Tunneling anisotropic magnetoresistence

The results presented above show that the computed anisotropy of TMR results exclusively from the anisotropy of tunneling in the AFM configuration. Thus, this anisotropy cannot explain the in-plane TAMR effect observed in the (Ga,Mn)As/GaAs/Ga,Mn)As structures,[13,14] *i. e.*, the difference in the resistance of

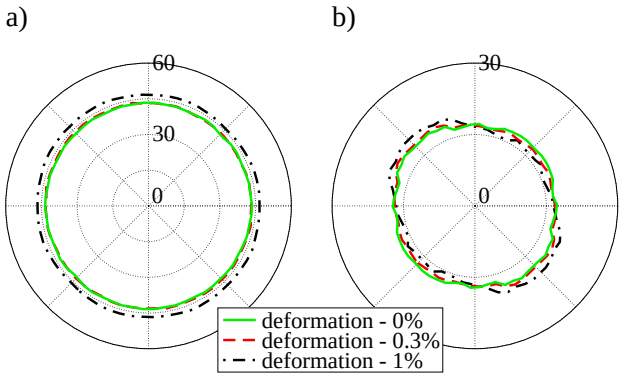

FIG. 11: [color on-line] Dependence of tunneling current on the direction of in-plane magnetization for (a) parallel (FM) and (b) antiparallel (AFM) magnetization orientations in p-$Ga_{0.92}Mn_{0.08}As$/$(GaAs)_4$/p-$Ga_{0.92}Mn_{0.08}As$ trilayer structures trigonally distorted along the [110] crystallographic axis; $p = 3.5 \times 10^{20}$ cm^{-3}.

the structures in FM configuration between the x and y directions. As stated before, we obtain only a very small difference in the FM tunneling current between the [110] and [010] direction. Although this anisotropy can be increased to about 15% by assuming a low hole concentration of $p = 1 \times 10^{19}$ cm^{-3} (compare Fig. 12), the depletion effects would not affect the anisotropy directions determined by the symmetry of the structure.

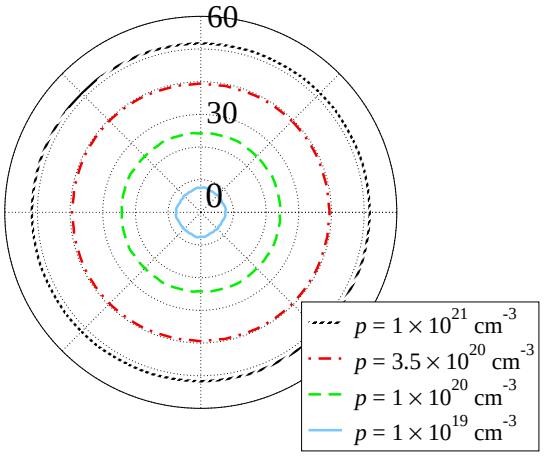

FIG. 12: [color on-line] Dependence of tunneling current on the direction of in-plane magnetization structures with parallel magnetization configuration (FM) for various hole concentrations in p-$Ga_{0.92}Mn_{0.08}As$/$(GaAs)_4$/p-$Ga_{0.92}Mn_{0.08}As$ trilayer structure; $p = 3.5 \times 10^{20}$ cm^{-3}.

However, the calculated tunneling current for magnetization vector perpendicular to the plane differs from the current calculated for the in-plane magnetization vector even for the FM configuration. Using the TAMR$_\perp$ ratio defined in Eq. (8), we have calculated the perpendicular TAMR for the (Ga,Mn)As/GaAs/(Ga,Mn)As and (Ga,Mn)As/AlAs/(Ga,Mn)As structures. The results are presented in Fig. 13. In the case of the GaAs spacer, for hole concentrations of about 1×10^{20} cm^{-3} a very small effect that weakly depends on the applied bias can be observed. Still, for small hole concentration we see a positive TAMR$_\perp$ of the order of 60%. The difference between the out-of-plane and in-plane resistances of the same sign and of about 12% was experimentally observed in Ref. 14. As shown in Fig. 13, again a higher barrier, *i. e.*, the AlAs spacer, should enhance the TAMR$_\perp$ effect.

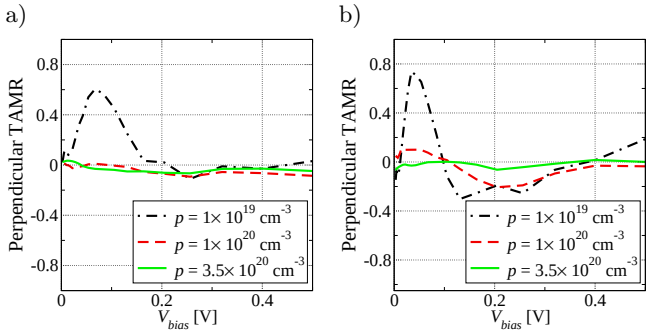

FIG. 13: [color on-line] Bias dependence of the TAMR$_\perp$ ratio for TMR structure consisting of two magnetic p-$Ga_{0.92}Mn_{0.08}As$ layers separated by (a) GaAs and (b) AlAs barrier layer; $p = 3.5 \times 10^{20}$ cm^{-3}.

V. SUMMARY

We have developed the model of quantum transport in spatially modulated structures of hole-controlled diluted ferromagnetic semiconductors, taking into account relevant features of the band structure within the tight-binding approximation. The model disregards disorder and effects of carrier–carrier interactions, so that it is applicable to the carrier density range and length scales, where localization effects are unimportant. The computation results presented in this and our previous papers[16,17] demonstrate that many of experimentally important effects, such as large magnitudes of both spin polarization of the tunneling current in Zener-Esaki diodes and TMR ratio in trilayer structures can be understood within the proposed model. Furthermore, the theory describes quantitatively a fast decay of the spin polarization of the current and TMR with the bias voltage without invoking inelastic processes. However, these processes together with heating of Mn spin subsystem may become crucial in the highest bias regime. The detail studies of anisotropy effects reveal the presence of C_{2v} symmetry in the magnitude of current spin polarization in the Zener-Esaki diode. This indicates a noticeable importance of inversion asymmetry terms specific to interfaces and zinc-blende structure in tunneling structures. These effects are not taken into account within the standard kp-type approaches. According to our findings, if strain is not excessively large, the dominant anisotropy appears when

the direction of magnetization changes from parallel to perpendicular to the current, in a full analogy to AMR. Finally, we have used the model to predict theoretical conditions for improving the performance of the studied devices. Our results indicate that an attempt to increase the electron concentration in the n-GaAs layer of the Zener-Esaki tunnel junction should pay off in an increase of the spin polarization of the current. For the trilayers, the calculations suggest that reducing barrier thickness and increasing barrier height may result in higher values of TMR and its slower decay with the applied bias.

Acknowledgments

We thank Hideo Ohno, Fumihiro Matsukura, Wim Van Roy, and Albert Fert for valuable discussions. This work was partly supported by the EC project NANOSPIN (FP6-2002-IST-015728). Computations were carried out exploiting resources and software of Interdisciplinary Center of Mathematical and Computer Modelling (ICM) in Warsaw.

[1] for a review on III-V diluted magnetic semiconductors, see, F. Matsukura, H. Ohno, and T. Dietl, in: *Handbook of Magnetic Materials*, vol. 14, edited by K. H. J. Buschow (North-Holland, Amsterdam, 2002) p. 1.

[2] M. Tanaka and Y. Higo, Phys. Rev. Lett. **87**, 026602 (2001).

[3] R. Mattana, J.-M. George, H. Jaffrés, F. N. van Dau, A. Fert, B. Lépine, A. Guivarch, and G. Jézéquel, Phys. Rev. Lett. **90**, 166601 (2003).

[4] D. Chiba, F. Matsukura, and H. Ohno, Physica E **21**, 966 (2004).

[5] M. Elsen, O. Boulle, J.-M. George, H. Jaffrés, R. Mattana, V. Cros, A. Fert, A. Lemaître, R. Giraud, and G. Faini, Phys. Rev. **73**, 035303 (2006).

[6] T. Dietl, H. Ohno, and F. Matsukura, Phys. Rev. B **63**, 195205 (2001).

[7] Y. Ohno, D. K. Young, B. Beschoten, F. Matsukura, H. Ohno, and D. D. Awschalom, Nature **402**, 790 (1999).

[8] M. Kohda, Y. Ohno, K. Takamura, F. Matsukura, and H. Ohno, Japn. J. Appl. Phys. **40** (Part 2), L1274 (2001); E. Johnston-Halperin, D. Lofgreen, R. K. Kawakami, D. K. Young, L. Coldren, A. C. Gossard, and D. D. Awschalom, Phys. Rev. B **65**, 041306(R) (2002); M. Kohda, Y. Ohno, F. Matsukura, and H. Ohno, Physica E **32**, 438 (2006).

[9] P. Van Dorpe, Z. Liu, W. Van Roy, V. F. Motsnyi, M. Sawicki, G. Borghs, and J. De Boeck, Appl. Phys. Lett. **84**, 3495 (2004).

[10] M. Kohda, T. Kita, Y. Ohno, F. Matsukura, and H. Ohno, Appl. Phys. Lett., in press.

[11] C. Gould, C. Rüster, T. Jungwirth, E. Girgis, G. M. Schott, R. Giraud, K. Brunner, G. Schmidt, and L. W. Molenkamp, Phys. Rev. Lett. **93**, 117203 (2004).

[12] R. Giraud, M. Gryglas, L. Thevenard, A. Lemaître, and G. Faini, Appl. Phys. Lett. **87**, 242505 (2005).

[13] C. Ruster, C. Gould, T. Jungwirth, J. Sinova, G. M. Schott, R. Giraud, K. Brunner, G. Schmidt, and L. W. Molenkamp, Phys. Rev. Lett. **94**, 027203 (2005).

[14] A. D. Giddings, M. N. Khalid, T. Jungwirth, J. Wunderlich, S. Yasin, R. P. Campion, K. W. Edmonds, J. Sinova, K. Ito, K.Y. Wang, D. Williams, B. L. Gallagher, and C. T. Foxon, Phys. Rev. Lett. **94**, 127202 (2005).

[15] A. G. Petukhov, A. N. Chantis, and D. O. Demchenko, Phys. Rev. Lett. **89**, 107205 (2002); L. Brey, Appl. Phys. Lett. **85**, 1996 (2004).

[16] P. Van Dorpe, W. Van Roy, J. De Boeck, G. Borghs, P. Sankowski, P. Kacman, J. A. Majewski, and T. Dietl, Phys. Rev. B **72**, 205322 (2005).

[17] P. Sankowski, P. Kacman, J. Majewski, and T. Dietl, Physica E **32**, 375 (2006).

[18] R. Oszwałdowski, J. A. Majewski, and T. Dietl, cond-mat/30605230.

[19] J.-M. Jancu, R. Scholz, F. Beltram, and F. Bassani, Phys. Rev. B **57**, 6493 (1998).

[20] J. Okabayashi, A. Kimura, O. Rader, T. Mizokawa, A. Fujimori, T. Hayashi, and M. Tanaka, Physica E **10**, 192 (2001).

[21] Aldo Di Carlo, P. Vogl, and W. Pötz, Phys. Rev. B, **50**, 8358, 1994.

[22] C. Strahberger and P. Vogl, Phys. Rev. B **62**, 7289 (2000).

[23] Aldo di Carlo, Semicond. Sci. Technol. **18**, R1 (2003).

[24] M. Sawicki, F. Matsukura, A. Idziaszek, T. Dietl, G. M. Schott, C. Ruester, C. Gould, G. Karczewski, G. Schmidt, and L. W. Molenkamp Phys. Rev. B **70**, 245325 (2004).

[25] M. Sawicki, K.-Y. Wang, K. W. Edmonds, R. P. Campion, C. R. Staddon, N. R. S. Farley, C. T. Foxon, E. Papis, E. Kaminska, A. Piotrowska, T. Dietl, and B. L. Gallagher Phys. Rev. B **71**, 121302(R) (2005).

[26] D. V. Baxter, D. Ruzmetov, J. Scherschligt, Y. Sasaki, X. Liu, J. K. Furdyna, and C. H. Mielke, Phys. Rev. B **65**, 212407 (2002); T. Jungwirth, J. Sinova, K. Wang, K.W. Edmonds, R. Campion, B. Gallagher, C. Foxon, Q. Niu, A. MacDonald, Appl. Phys. Lett. **83**, 320 (2003).